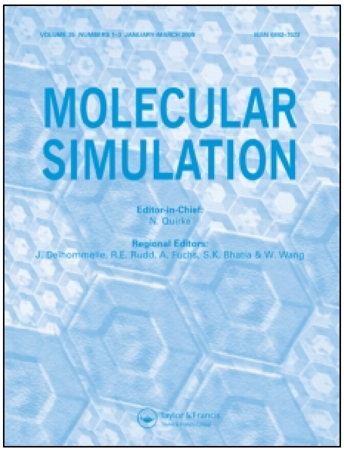

Molecular Simulation
Publication details, including instructions for authors and subscription information:
http://www.informaworld.com/smpp/title~content=t713644482

The effect of flexibility on thermodynamic and structural properties in methane hydrates

Florianne Castillo-Borja[a]; Richart Vázquez-Román[b]; Ulises Bravo-Sánchez[a]
[a] Departamento de Ingeniería Química y Bioquímica, Instituto Tecnológico de Aguascalientes, Aguascalientes, México [b] Departamento de Ingeniería Química, Instituto Tecnológico de Celaya, Celaya, México

To cite this Article Castillo-Borja, Florianne , Vázquez-Román, Richart and Bravo-Sánchez, Ulises(2008) 'The effect of flexibility on thermodynamic and structural properties in methane hydrates', Molecular Simulation, 34: 7, 661 — 670
To link to this Article: DOI: 10.1080/08927020802036062
URL: http://dx.doi.org/10.1080/08927020802036062

Molecular Simulation
Vol. 34, No. 7, June 2008, 661–670

The effect of flexibility on thermodynamic and structural properties in methane hydrates

Florianne Castillo-Borja[a]*, Richart Vázquez-Román[b] and Ulises Bravo-Sánchez[a]

[a]*Departamento de Ingeniería Química y Bioquímica, Instituto Tecnológico de Aguascalientes, Aguascalientes, México;*
[b]*Departamento de Ingeniería Química, Instituto Tecnológico de Celaya, Celaya, México*

(Received 10 January 2008; final version received 6 March 2008)

The purpose of the present study is to compare two different schemes for treating the intramolecular degrees of freedom in molecular dynamics simulation of methane hydrates by studying their effect on the simulated properties like energy, density and radial distribution functions at different thermodynamics conditions. The first scheme supposes molecules with rigid geometry and resembles the assumption made by van der Waals and Platteeuw of a lattice which is not distorted by guest molecules. The second scheme supposes a more realistic description from the hydrate by introducing translational and rotational degrees of freedom. The NPT molecular dynamic simulations include temperature ranges from 40 to 200 K for two different pressure conditions, 0.1 and 500 MPa. The results show that increments of temperature increase the energy and decrease the density of the hydrate in both models, rigid and flexible. The effect of temperature on the lattice parameter agrees with the experimental behaviour reported in other studies. The radial distribution functions showed that the hydrate with flexible molecules presents major distortion with regard to the rigid model. However, the radial distribution functions in both rigid and flexible models reproduce the experimental peaks at the same distance. In general, the effect of flexibility concerns in major measure the thermodynamic properties in comparison with the structural properties analysed in this work.

Keywords: methane hydrate; molecular dynamics; rigid and flexible molecules; radial distribution functions

1. Introduction

Hydrates are inclusion compounds in which molecules of water configured cages that are stabilised by guest molecules such as methane, ethane, carbon dioxide, or some other molecule small enough to occupy the interior of these cages [1]. Hydrates are ice-like crystalline solids and their cavities are formed by hydrogen bonding of the water molecules. Industrial interest in these compounds appeared because they represent a danger when they are formed in the pipes; for instance, during the oil and gas production. Thus, any strategy of risk control in the industry should include the knowledge of frontiers in thermodynamic stability for phase hydrate regions. In addition, a considerable geophysical interest in methane hydrates has emerged from the fact that existing methane hydrates in the permafrost region and at the bottom of the oceans of several countries are considered an important energy reserve. More recently, several theoretical and experimental studies have been carried out to understand the thermodynamic stability, to estimate structural and dynamic properties and to analyse the effect on the climate and the stability of the marine floor of methane hydrates [2–5].

The most typical crystalline structure of methane hydrates is the one called type sI. The unit cell of structure sI has a cubic shape with 12 Å of length, consists of 46 hydrogen-bonded water molecules and up to eight methane molecules occupying both small and large cavities in a ratio of 1:3. The small cavities of sI are pentagonal dodecahedral cages (5^{12}) and the large cavities are tetracaidecahedral cages ($5^{12}6^{2}$). Methane hydrates are known to exist at temperatures from 150 to 320 K and pressures from 0.01 up to 1000 MPa with more typical occupations of 95 and 50% for the large and small cavities, respectively [1].

Previous research on hydrates has been focused on solving the phase equilibrium problem where pressure, temperature and the composition mainly in the gas phase were also measured to verify estimations. The main tool to calculate fugacities and compositions of the hydrate phase involved in a multiple phase equilibrium evaluation, gas–ice- and gas–water-hydrate, is the theory developed by van der Waals and Platteeuw [6]. This theory assumes that the guest molecules inside cages of water molecules provide thermodynamic stability to the configuration that is even more stable than the ice or pure water. The theory was developed

---

*Corresponding author. Email: floriannecb@gmail.com

ISSN 0892-7022 print/ISSN 1029-0435 online

DOI: 10.1080/08927020802036062
http://www.informaworld.com

under three main considerations: the cavities of the lattice do not allow multiple occupation to the guest, the effect of interactions guest–guest is negligible and the interactions guest–water are relatively weak as to just consider the interactions of the molecules of water near to the guest molecules.

The main objective in several studies of molecular simulation has been to demonstrate the validity of the assumptions of the van der Waals and Platteeuw theory [3,7,8]. These simulations have used different types of non-polarisable intermolecular potentials with both rigid and flexible geometries to describe the molecules of water behaviour. In the case of methane molecules the most used approach has been to consider them as spherical molecules with just a single site of interaction of type Lennard-Jones. Rodger [8] calculates the configurational energy and radial distribution functions for methane hydrates using simulations NVT at 145, 200, 220, 240, 260 and 270 K with different proportions of the cavities occupied. In his work, water molecules are described as rigid and water–water intermolecular interactions are described by the simple point charge model SPC according to Berendsen et al. [9], and a type of Lennard-Jones potential for the water–methane and methane–methane interactions. Chialvo et al. [7] compared the effect of three types of potentials for the water, all with rigid geometry, in the calculation of thermo-physical and structural properties of methane hydrates at 270 K and 5 MPa and different compositions in simulations NPT. The potentials used in that study for the water were the SPC, SPC/E [10] and the TIP5P [11] whereas the methane was modelled as a rigid molecule of five interaction sites of type Lennard-Jones. Recently, Sizov et al. [3] performed simulations with the grand canonical ensemble Monte Carlo method (GCMC) to calculate several occupancy isotherms at 200, 210, 220, 230, 235, 240, 250 and 260 K for methane hydrates with flexible and rigid hydrogen-bonded network forming the clathrate cages. This study describes the water interactions with the SPC/E model along with the united-atom (UA) Lennard-Jones model for methane interactions [12]. It becomes clear from the above researches that there is a need of more realistic description for the interactions water–guest, guest–guest and water–water, as well as a bigger emphasis in the geometry of the molecules in the lattice to allow more flexibility.

More recently, Jiang et al. [2] have improved the molecular description of methane hydrates by using two polarisable potentials for the water, the AMOEBA [13] and the COS/G2 [14] models, and a combination of an electrostatic potential and the Lennard-Jones for the methane. Their description included both rigid and flexible cases in the two types of molecules. The results obtained included some of the radial distribution functions and the vibrational spectrum at 270 K and 20 bar, as well as the effect of temperature on the lattice constants using simulations NPT. Overall the simulations with the AMOEBA model have better agreement with experiment results in contrast with COS/G2 model. However, the analysed simulation times were limited to short times of 100 and 500 ps due to the computational demand required in AMOEBA and COS/G2, respectively.

In this work, the hydrate models behaviour having flexible and rigid geometry is compared based on molecular dynamics simulations. The numerical results agree with experimental values in the radial distribution function and the lattice parameter. The rigid geometry resembles the assumption made by van der Waals and Platteeuw of a lattice that is not distorted by guest molecules. On the other hand, the flexible geometry provides a more realistic description from the hydrate introducing translational and rotational degrees of freedom, considering the possibility of stretching bonds as well as allowing flexion of the angles in the molecules of water and methane. The results obtained include the temperature and pressure effect on the hydrate lattice parameter in a range of temperatures of 40–200 K and pressures of 0.1 and 500 MPa. For the two analysed models, the volume of the hydrate increases when the temperature is increased in agreement to the reported experimental results of thermal expansivity [15]. In the same way, the effect of the hydrate geometry on radial distribution functions is analysed for the interactions water–water and methane–methane.

2. Simulation procedures

The phase space in molecular dynamics simulations of a system of N atoms consists of the position coordinates and velocities of each particle. For a given initial state, the phase space is evolved by solving the Newton equations of movement during a period of time in which the values of atomic positions and velocities are stored for their later statistical treatment and to calculate several properties of the system. The Newton equation for each atom is a differential equation that is solved usually with some finite differences method. In this work, the velocity-Verlet method is used because it appropriately handles the atomic velocities and minimises the rounding error [16].

The typical integration time step used in the solution of Newton equations can be of several femtoseconds (fs); however, the highest frequency motions in the system place the effective limit as to how large the time step can be for the simulations [17]. Because the highest frequency motion is generally associated with bond vibrations, a time step of 0.4 fs was used in the flexible molecule simulations to assure the stability of the time discretisation method. In the rigid molecule simulations, the impositions of algebraic constraints that fix bonds and angles remove the associated rapid vibrational modes, enabling the use of longer time steps without substantially altering important physical characteristics of the motion. The size of the integration step used in this case was 0.8 fs. For the rigid and flexible molecule simulations the length of the simulations was 320 ps with 200 ps for equilibration of the system.

Simulations were carried out for systems containing eight totally occupied unit cells of methane hydrate ($2 \times 2 \times 2$) type sI. The position of the oxygen atoms and the centre of mass for guest molecules in the unit cell for our starting configurations were taken from the X-ray analysis of ethylene oxide hydrate by McMullan and Jeffrey [18]. The protons of water molecules were placed according to the Bernal–Fowler rules [19] and oriented in such a way that there is no net dipole moment in the unit cell. The length of the simulation box was 24.06 Å. This size of the simulation cell has been used by others and it allows the system to be equilibrated to obtain properties with standard deviations in a rather short simulation time [2,3,7,20]. Each system contains 368 water molecules and 64 methane molecules and the composition of each system remains constant during the whole simulation. Periodic boundary conditions were used in the three dimensions of the simulation box, i.e. the calculation algorithm assumes that the simulation box is indefinitely replied to avoid surface effects. The Berendsen weak-coupling algorithm was used to keep pressure and temperature constants [21]. These methods maintain the temperature oscillating around a specific value by scaling of velocities, while the pressure is controlled through the scaling of the atomic coordinates and volume of the simulation box. Thus, the number of molecules, pressure and temperature remained constant during all simulations.

The static properties produced with the molecular dynamics algorithm were energy configurational, density and radial distribution functions $g_{ij}(r)$ for pairs oxygen–oxygen, oxygen–hydrogen and hydrogen–hydrogen in molecules of water and radial distribution functions for carbon–carbon in the methane molecules. It is possible to measure $g_{ij}(r)$ experimentally with neutron scattering or X-ray scattering diffraction data. The $g_{ij}(r)$ indicate the probability to find a pair of atoms separated by a distance r, with respect to the probability expected for a completely random distribution with the same density [22]. The radial distribution function can be evaluated through the following equation:

$$g_{ij}(r) = \frac{\langle n_j(r+\delta r)\rangle}{4\pi\rho_j \int r^2 \mathrm{d}r} \tag{1}$$

where $< n_j(r+\delta r) >$ is the average number of atoms j that are separated from atom i by distances between r and $r+\delta r$ and ρ_j is a mean density of atoms j in the system.

The equations of motion are applied to each atom and the net force acting on a given atom i is obtained from the gradient of a potential or force field established by its interaction with all the other atoms in the system during an instantaneous time. In this work, two alternatives are considered to describe this force field in the molecular system. In the first case, molecules of water and methane are considered totally flexible, i.e. both intermolecular and intramolecular interactions are allowed. In the second case, rigidity is considered in the two types of molecules so that only intermolecular interactions remain. Intramolecular vibrations can be rejected for temperatures close to the environment because $h\omega_i/2\pi \gg k_{\mathrm{B}}T$, where h is the Planck constant, ω_i is the angular frequency of the i-normal mode of vibration, k_{B} is the Boltzmann constant and T is the temperature. However, the molecular flexibility can become important in high temperatures and pressures producing results more similar to the experimental values [23].

There are several analytic forms reported in the literature for flexible force fields of water and methane. The model TJE [24] is used here to describe the potential of molecules of water and the OPLS-AA [25] for methane molecules. Both models appropriately predict the properties of pure substances in wide ranges of temperature and pressure. The model TJE considers three interaction sites corresponding to each atom of the water molecule and a charge is assigned to each atom to reproduce the dipolar moment of the water molecule in liquid phase. The model TJE considers a Lennard-Jones potential centred in the oxygen atom as in the model SPC and the intramolecular potential is described through harmonic forms for all vibrational terms. The model OPLS-AA has an interaction site in each atom of the methane molecule that allows more flexibility for charge distributions and the calculation of the energy for flexion effects and stretching. The equation for the model TJE and OPLS-AA defines the variation of the potential energy of the system due to intermolecular non-bonded interactions. It consists of Lennard-Jones potential added to an electrostatic potential and, for the calculation of long-range electrostatic forces, the reaction field method [26] was used:

$$\begin{aligned} u(r_{ij})_{\text{inter}} = \sum_i \sum_{j>i} \Bigg(& 4\varepsilon_{ij}\left[\left(\frac{\sigma_{ij}}{r_{ij}}\right)^{12} - \left(\frac{\sigma_{ij}}{r_{ij}}\right)^{6}\right] \\ & + \frac{1}{4\pi\varepsilon_0}\frac{q_i q_j}{r_{ij}}\left[1 + \frac{\varepsilon_{\mathrm{RF}}-1}{2\varepsilon_{\mathrm{RF}}+1}\left(\frac{r_{ij}}{r_{\mathrm{c}}}\right)^{3}\right]\Bigg) \end{aligned} \tag{2}$$

where σ_{ij} and ε_{ij} are Lennard-Jones parameters, r_{ij} is the distance between two sites i and j, q_i and q_j are electrostatic charges in sites i and j, r_{c} is the cutoff radius equivalent to half the length of the simulation box, ε_0 is the permittivity of the free space and $\varepsilon_{\mathrm{RF}}$ is the external dielectric constant defining the reaction field whose value is fixed to infinite to represent conducting boundary conditions. The value of $\varepsilon_{\mathrm{RF}}$ is usually set to approximately ε_0 though any value between $\varepsilon_0 \leq \varepsilon_{\mathrm{RF}} \leq \infty$ is acceptable for moderately and highly polar substances [26]. For consistency, long-range correction was made for the Lennard-Jones term of the intermolecular potential described in Equation (2).

For the model TJE and OPLS-AA, flexibility is achieved by using bond stretching and angle bending terms for all bonds and angles in the water and methane molecules. The equations to calculate the variation in the intramolecular potential energy, due to the positions of the atoms in the molecules, are the following harmonic oscillators:

$$u(r_{ij})_{\mathrm{intra}} = \sum_{\text{all bonds}} \frac{1}{2} k_{\mathrm{b}} (r_{ij} - r_0)^2 + \sum_{\text{all angles}} \frac{1}{2} k_{\theta} (\theta - \theta_0)^2 \tag{3}$$

where k_{b} is the force constant for bond stretching between atoms i and j, r_{ij} and r_0 are the instantaneous and equilibrium bond lengths, k_θ is the force constant for the angle bending between atoms i, j and k, θ and θ_0 are the instantaneous and equilibrium angles.

The values of the constants used in Equations (2) and (3) for the model TJE and OPLS-AA are shown in Table 1. Parameters in Table 1 are used with the Lorentz–Berthelot combination rules to determine the Lennard-Jones parameters in the case of the non-electrostatic interactions between molecules of water and methane.

To model rigid geometry in hydrates, the simple point charge model SPC [9] is used. This model is a simple nonpolarisable water intermolecular potential with rigid geometries. This model provides an effective potential where all its parameters are obtained from thermodynamic data where the average effect of any intramolecular movement is included. The SPC model contains punctual charge in the oxygen and hydrogen of the water molecule interacting through an electrostatic potential. Each atom of oxygen in the water interacts through a Lennard-Jones potential. A Lennard-Jones potential is used for methane with adjusted parameters for each interaction type considering that the molecule is rigid with five interaction sites corresponding to each type of atom in the methane [7]. Equation (2) is used to calculate the potential energy of the system in the case of the rigid geometry and it is applied for all water and methane molecules of the hydrate. Lennard-Jones parameters as well as electrostatic charges involved in the rigid model calculation are given in Table 2. The Lorentz–Berthelot combination rule was used to determine the parameters of Lennard-Jones potentials between the water and methane molecules.

Table 1. Parameters for water and methane in the flexible structure.

Water		Methane	
Parameter	Value	Parameter	Value
θ_0 H—O—H	109.47°	θ_0 H—C—H	107.8°
r_0 O—H	1 Å	r_0 C—H	1.09 Å
k_θ H—O—H	46,065 K/rad^2	k_θ H—C—H	33,212.9 K/rad^2
k_{b} O—H	557,711.2 K/Å^2	k_{b} C—H	342,193.9 K/Å^2
$\varepsilon_{\mathrm{OO}}$	78.2 K	$\varepsilon_{\mathrm{CC}}$	33.2 K
σ_{OO}	3.166 Å	σ_{CC}	3.5 Å
q_{O}	−0.82 e	$\varepsilon_{\mathrm{HH}}$	15.09 K
q_{H}	0.41 e	σ_{HH}	2.5 Å
		q_{C}	−0.24 e
		q_{H}	0.06 e

The length of covalent bonds as well as internal angles of rigid water and methane molecules were kept in the equilibrium condition (Table 2) using the RSHAKE method [27] with a tolerance of 10^{-5}. This procedure was developed to model molecular dynamics in systems where certain degrees of freedom such as bond lengths or angles remain constant. The method was implemented for the first time by Ryckaert et al. [28] using an undetermined group of multipliers to represent the forces directed along the bonds to keep the angles and bond lengths as a constant. In this technique, the equations of motion are firstly integrated in absence of the constraint forces and then their magnitudes are determined to correct the atomic positions. Andersen [27] iteratively solves the constraints one by one adjusting the atomic coordinates involved in each bond and angle. The procedure is iteratively applied until all the constraints are satisfied within a certain tolerance.

3. Results and discussion

The effect of flexibility in molecules related to thermodynamic and structural properties is the main

Table 2. Parameters for water and methane in the rigid structure.

Water		Methane	
Parameter	Value	Parameter	Value
θ_0 H—O—H	109.5°	θ_0 H—C—H	109.5°
r_0 O—H	1 Å	r_0 C—H	1.04 Å
$\varepsilon_{\mathrm{OO}}$	78.2 K	$\varepsilon_{\mathrm{CC}}$	48.72 K
σ_{OO}	3.166 Å	σ_{CC}	3.351 Å
q_{O}	−0.82 e	$\varepsilon_{\mathrm{HH}}$	6.79 K
q_{H}	0.41 e	σ_{HH}	2.868 Å
		$\varepsilon_{\mathrm{CH}}$	20.55 K
		σ_{CH}	3.024 Å

Table 3. Results of thermodynamic properties at 0.1 MPa of pressure.

	U (kJ/mol)		ρ (g/cm^3)	
T (K)	Rigid	Flexible	Rigid	Flexible
40	$-48{,}504.64 \pm 4.11$	$-50{,}723.06 \pm 3.79$	$1.004555 \pm 4.4 \times 10^{-5}$	$1.028123 \pm 3.4 \times 10^{-5}$
80	$-46{,}790.00 \pm 4.46$	$-47{,}576.30 \pm 4.72$	$0.994742 \pm 4.5 \times 10^{-5}$	$1.015868 \pm 5.1 \times 10^{-5}$
120	$-44{,}948.36 \pm 5.14$	$-44{,}208.87 \pm 5.41$	$0.982627 \pm 5.8 \times 10^{-5}$	$1.003124 \pm 6.2 \times 10^{-5}$
160	$-42{,}812.95 \pm 5.15$	$-40{,}685.19 \pm 6.04$	$0.967680 \pm 7.0 \times 10^{-5}$	$0.987323 \pm 8.2 \times 10^{-5}$
200	$-40{,}495.65 \pm 6.03$	$-36{,}887.10 \pm 7.40$	$0.949179 \pm 9.3 \times 10^{-5}$	$0.968605 \pm 1.08 \times 10^{-4}$

issue analysed in this work. Previous studies about structural properties of flexible models for water under room temperature conditions have demonstrated that inclusion of flexibility causes small increments in the first two peaks of the oxygen–oxygen radial distribution function (gOO) in comparison with the results of rigid models [24,29]. In addition, simulations of flexible water show a bigger potential energy in comparison with the rigid model [29]. The explanation of these results is based on the different molecular dipole and quadrupole moments assigned to each model for water. The flexibility of the water molecule causes an increase in the molecular dipole moment compared with a rigid molecule leading to stronger bonds in molecules of water with its surroundings.

3.1 Thermodynamic properties

The thermodynamic properties of methane hydrates obtained from NPT simulations with both rigid and flexible models are outlined in Table 3 at 0.1 MPa. Table 4 presents the results for NPT simulations at 500 MPa. These conditions of pressure were selected because of the possibility suggested in recent years to transport natural gas in the form of hydrate at 0.1 MPa [30] whereas the condition of 500 MPa was selected to contrast the results with experimental results of temperature dependence of the unit cell parameters for methane hydrate [15]. Both pressure values represent the extremes of the most studied region in the last years for methane hydrate.

In general, it is observed that increments in the temperature produce a decrease of the density as the energy configurational increases in the two models for both pressure conditions. The effect of pressure on the energy is hardly observed in both schemes; however, the pressure affects significantly the density of the hydrate. In the case of rigid structure, there is a minor increase in the potential energy when the temperature is increased with respect to the flexible model. Furthermore, the rigid structure presents smaller density in comparison to the flexible structure in all our studies. In fact, Zhang et al. [31] analysed water–methane mixtures and they found a similar response in energy and density when the temperature was changed within the interval of 270–300 K and 80 MPa. In their case, NPT molecular dynamics simulations were carried out using rigid geometry for the molecules with potential TIP4P for water and a Lennard-Jones for methane and water–methane interactions. More recently, Jiang et al. [2] have compared their results of potential energy in methane hydrates with those obtained by others in NVT molecular dynamics with rigid geometries and different potentials for water. The temperatures analysed were 50, 125 and 200 K and the same increase tendency was observed in the energy while increasing the temperature for all analysed potentials. Unfortunately, there is a lack of experimental data for density and energy as to compare this numerical result.

3.2 Radial distribution functions

The radial distribution functions gOO, gOH and gHH are commonly used to analyse structures of aqueous solutions. They can be obtained experimentally starting

Table 4. Results of thermodynamic properties at 500 MPa of pressure.

	U (kJ/mol)		ρ (g/cm^3)	
T (K)	Rigid	Flexible	Rigid	Flexible
40	$-48{,}225.92 \pm 3.18$	$-50{,}409.05 \pm 3.63$	$1.034549 \pm 8.0 \times 10^{-6}$	$1.056611 \pm 1.9 \times 10^{-5}$
80	$-46{,}459.59 \pm 4.37$	$-47{,}259.42 \pm 4.61$	$1.025940 \pm 2.9 \times 10^{-5}$	$1.045369 \pm 2.1 \times 10^{-5}$
120	$-44{,}659.99 \pm 4.55$	$-44{,}037.32 \pm 5.12$	$1.016507 \pm 1.3 \times 10^{-5}$	$1.036564 \pm 2.9 \times 10^{-5}$
160	$-42{,}726.40 \pm 5.21$	$-40{,}697.75 \pm 5.80$	$1.006398 \pm 1.6 \times 10^{-5}$	$1.026002 \pm 3.9 \times 10^{-5}$
200	$-40{,}685.06 \pm 5.40$	$-37{,}142.33 \pm 6.89$	$0.995413 \pm 2.0 \times 10^{-5}$	$1.015188 \pm 4.9 \times 10^{-5}$

from diffraction of neutrons studies. To understand the shape of this type of function, consider an atom in the origin, $r = 0$, for the calculation of the radial distribution function while all other atoms in the system are orderly accommodated around this atom. In the case of solids, it is very likely that the first layer of atoms surrounding the central atom is accommodated at a distance r that corresponds to the first peak showed in the radial distribution function. This first layer tends to exclude the following layer of neighbours in a region so that $g(r)$ has a value smaller than the unity in this region. Then, the following layer of neighbors is allocated at some distance to produce the second peak in the $g(r)$ function. Thus, there is a distance where the atoms are not affected by the presence of the central atom and the $g(r)$ takes the unit value. In the case of solids such as the hydrate, the peaks of the $g(r)$ are more defined and slender in comparison with the peaks of a liquid. Since the layers of neighbouring atoms are very well defined in the solid, the $g(r)$ has a zero value between each peak representing to the first layers of atoms and it latter presents oscillations around the unity value.

Thus, the structure of the water in the hydrate is described by the radial distribution functions of gOO, gHH and gOH. These radial distribution functions can be observed for the water–water interactions obtained from NPT simulations at different pressure and temperature conditions as indicated in Tables 3 and 4. The effect of pressure produces a similar behaviour on the radial distribution functions so that only the case of 0.1 MPa is analysed. Figure 1(a),(b) shows that the position of the peaks for the gOO function is hardly different among the different temperatures. A similar result is also observed in the gOH functions given in Figure 2(a),(b). However, a reduction in the height of the peaks can be observed in Figures 1(a),(b) and 2(a),(b) for rigid and flexible molecule models when increasing the temperature. The effect of temperature on the gOO and gOH functions reflects bigger mobility of the water molecules when the temperature increases for both molecule models.

In addition, the effect of inflexibility in the molecules produces more lengthened and narrow peaks for the different radial distribution functions, mainly in the first and second pick. This suggests that the organisation of the water molecules of the lattice in the hydrate is less structured when the molecules are considered flexible. When inflexibility in the molecules is allowed, a better accommodation of the molecules is allowed and, hence, the lattice cannot be really distorted. The first layer of oxygen surrounding the central oxygen is represented by the first peak of the gOO function, which appears in 2.7 Å. The second layer of neighbouring oxygen appears at 4.6 Å and a third layer appears at 6.5 Å. Although other peaks appear beyond 6 Å, the deviations respect to the unit value in the radial distribution function

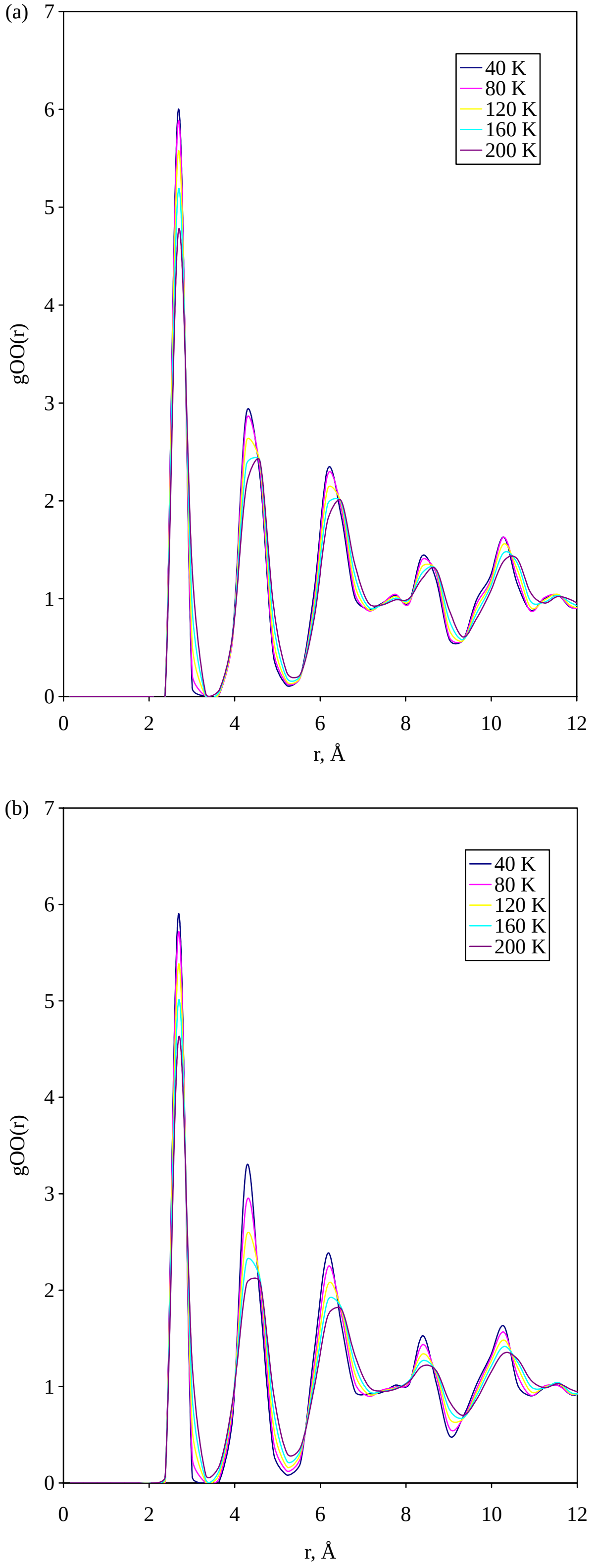

Figure 1. (a) Radial distribution functions for oxygen–oxygen in water at 0.1 MPa and different temperatures for a rigid structure. (b) Radial distribution functions for oxygen–oxygen in water at 0.1 MPa and different temperatures for a flexible structure.

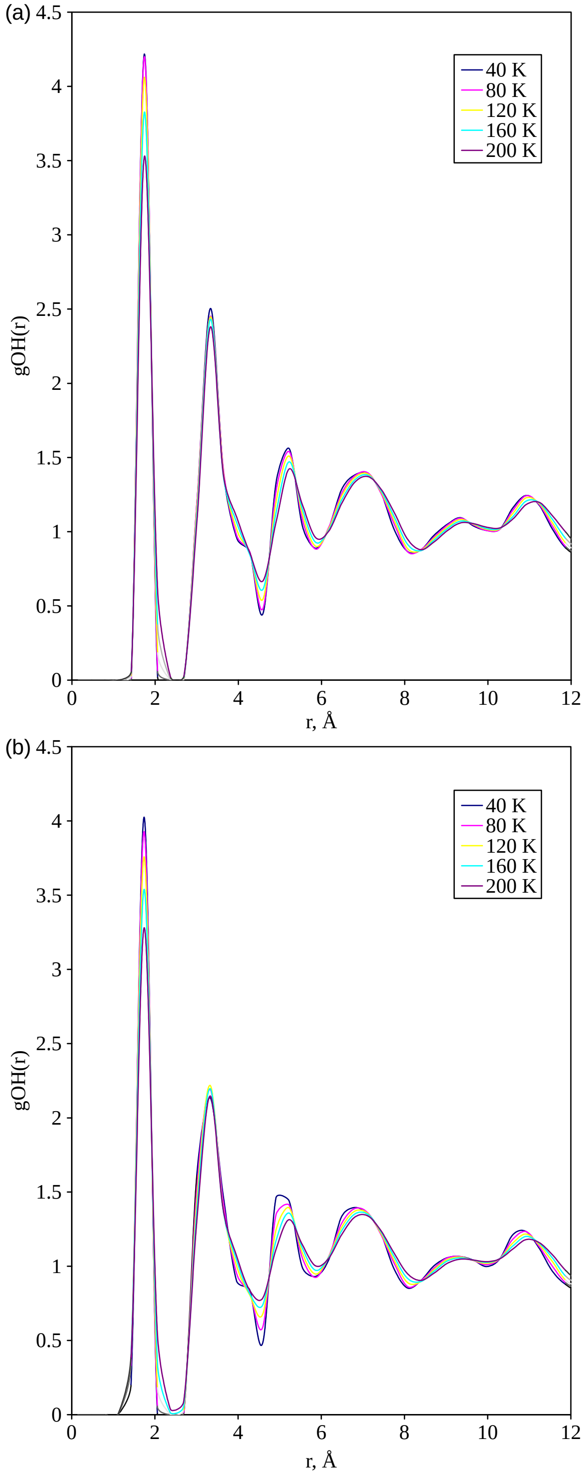

Figure 2. (a) Radial distribution functions for oxygen–hydrogen in water at 0.1 MPa and different temperatures for a rigid structure. (b) Radial distribution functions for oxygen–hydrogen in water at 0.1 MPa and different temperatures for a flexible structure.

is insignificant. Figure 2(a),(b) shows that the first peak appears in 1.74 Å. This peak corresponds to the average length of the hydrogen bonds formed in the water molecules. The experimental value of this type of bond among molecules of liquid water is 1.85 Å [31]. This result suggests that the hydrogen bonds in the hydrate are shorter due to the packing of water molecules.

The gHH functions for rigid and flexible hydrates at 0.1 MPa and different temperatures are shown in Figure 3(a),(b). In this case, a decrease in the height of the peaks, as in the gOO and gOH functions, is observed when the temperature is increased for both models. In addition, it is observed that the rigid structure presents a bigger height in the first peak, suggesting the existence of more hydrogen atoms surrounding the central hydrogen for this molecule model in comparison with the flexible model. The average distance between central hydrogen and the closest neighbour hydrogen is 2.38 Å in accordance with the Figure 3(a),(b). Zhang et al. [31] have found that this peak appears approximately at the same distance for liquid mixtures containing water and methane at 270 and 300 K.

Figure 4(a),(b) show the radial distribution functions to characterise the structure of methane in different simulations analysed in this study. In general, it is observed that the peaks are higher in the rigid geometry and diminishes when the temperature increases, which is consistent with the radial distribution functions gOO and gOH of water. It consequently gives better defined structures of the hydrate. Figure 4(a),(b) shows the average distance of a couple of carbons in the methane for both flexible and rigid geometries. The existence of two very well defined picks at 6.8 and 10.9 Å is clearly observed. The height and position of these picks agree with those reported for methane hydrates at 200 K and 20 bar [2].

The maxima and minima positions of the gOO and gCC positions obtained in the rigid geometry simulation at 200 K and 0.1 MPa are compared to experimental values at 293 K and 14.5 MPa [32] in Tables 5 and 6. Radial distribution functions were obtained from neutron diffraction data through the empirical potential structure refinement technique [33], which allows detailed studies of structural properties. Differences between flexible and rigid models in predicting the peaks and minima positions are negligible and the comparison with experimental values is acceptable. Tables 5 and 6 show the numerical results for the rigid model and the experimental values.

3.3 *Lattice parameter*

It is believed here that knowing the change in the hydrate volume with a change in temperature can help to understand the microscopic and macroscopic behaviour of hydrates. Hydrates have a thermal expansivity bigger than hexagonal ice, in particular below 200 K, due to the vibrational movements of the guest molecules and their interactions with the lattice. Though the van der Waals

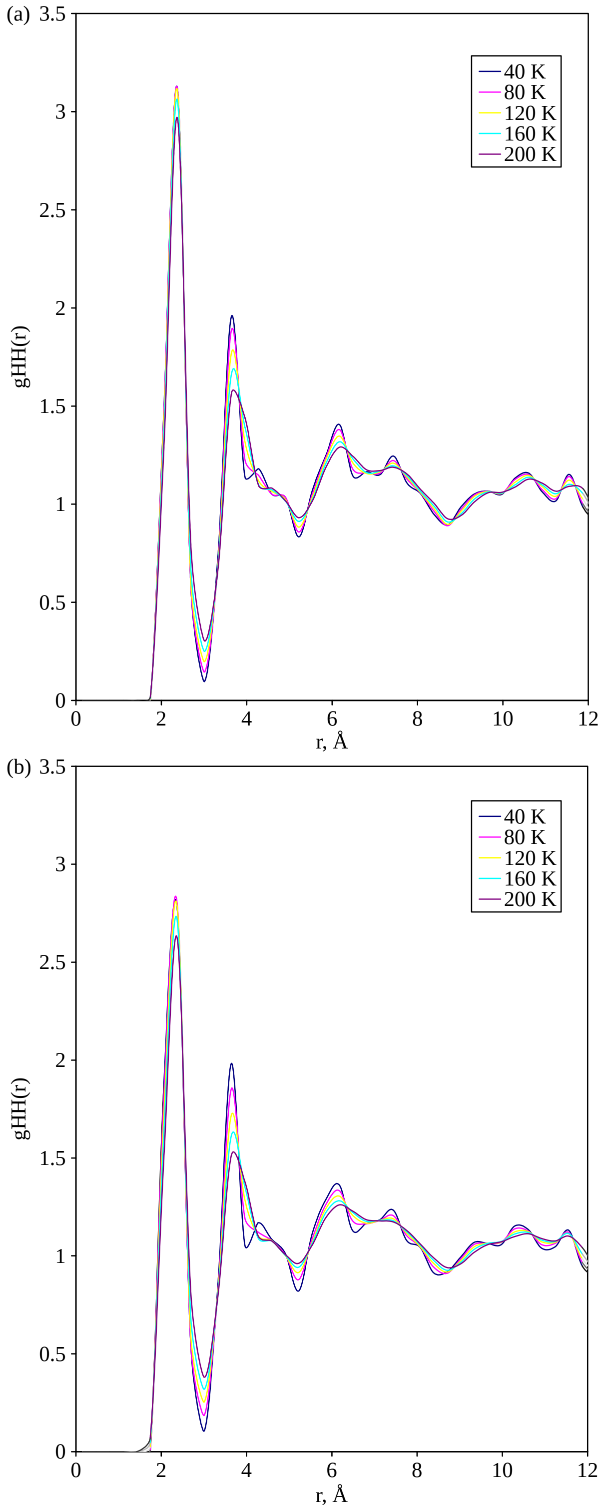

Figure 3. (a) Radial distribution functions for hydrogen–hydrogen in water at 0.1 MPa and different temperatures for a rigid structure. (b) Radial distribution functions for hydrogen–hydrogen in water at 0.1 MPa and different temperatures for a flexible structure.

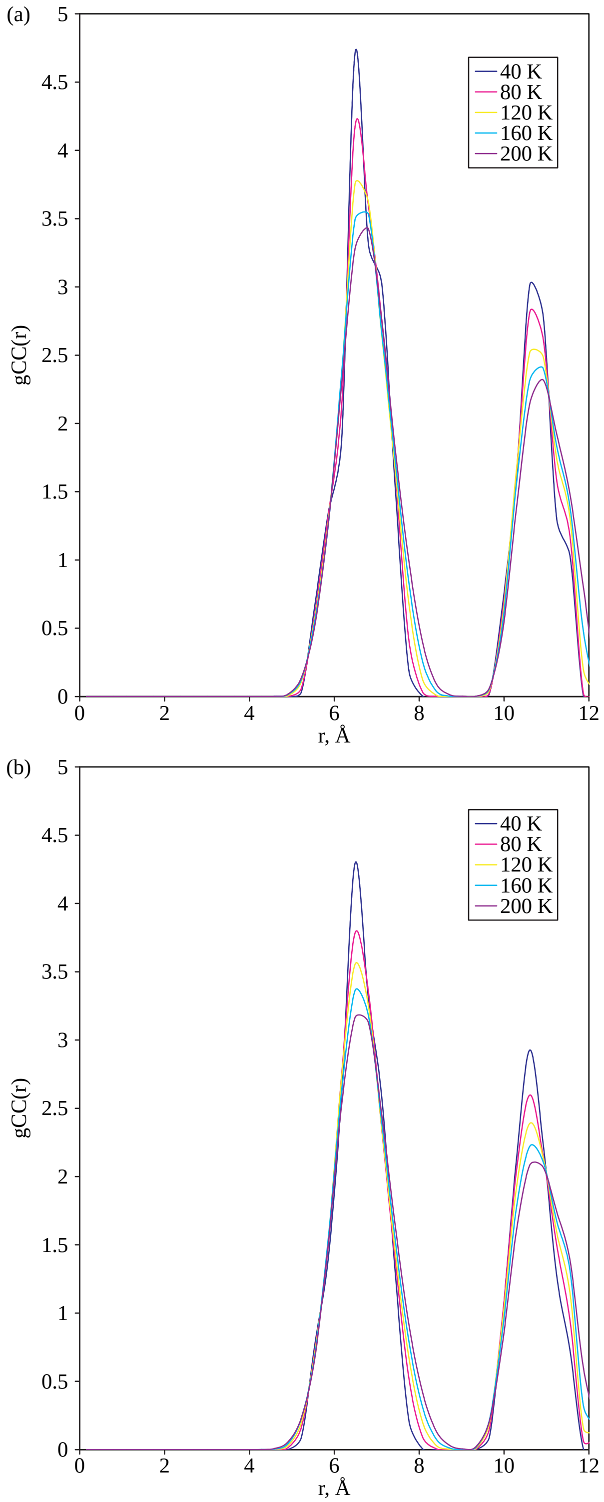

Figure 4. (a) Radial distribution functions for carbon–carbon in methane at different temperatures for a rigid structure. (b) Radial distribution functions for carbon–carbon in methane at different temperatures for a flexible structure.

Table 5. Comparison of oxygen–oxygen pair distribution function.

Model	First maximum position (Å)	First minimum position (Å)	Second maximum position (Å)	Second minimum position (Å)	Third maximum position (Å)
Rigid	2.7	3.3	4.6	5.5	6.5
Exptl [32]	2.6	3.2	4.5	5.3	6.1

Table 6. Comparison of carbon–carbon pair distribution function.

Model	First maximum position (Å)	First minimum position (Å)	Second maximum position (Å)
Rigid	6.8	9.0	10.9
Exptl [32]	6.2	9.0	11.1

and Platteeuw theory assumes no distortion in the lattice, several studies have demonstrated that combination of temperature, pressure and size effects in the guest can induce changes in volume [15,34]. These changes in the hydrate volume are rather small but they can lead to meaningful differences in the hydrate formation conditions when using the van der Waals and Platteeuw theory. A great number of hydrates with structures sI and sII, with very few exceptions, have a common thermal expansivity irrespectively of the guest's type according to observations based on diffraction studies with X-rays [34]. Figure 5 shows the lattice parameter of the unit cell obtained for the different simulations indicated in Tables 3 and 4. The distortion in the flexible structure is bigger than the one obtained in the rigid one as indicated in the results of radial distribution functions. Furthermore, the hydrate at 500 MPa is less deformed than in the 0.1 MPa case. A polynomial expression has been proposed to describe the lattice parameter variation as a function of temperature for a valid range of 86–267 K and 500 MPa [15]. The increase of the lattice parameter with the temperature observed in Figure 5 agrees in its behaviour with the experimental study for the thermal expansivity of methane hydrates at 500 MPa [15]. However, it is observed that the lattice parameter at 500 MPa for the rigid model has an average error of 2.15% whereas the flexible model has 2.8%.

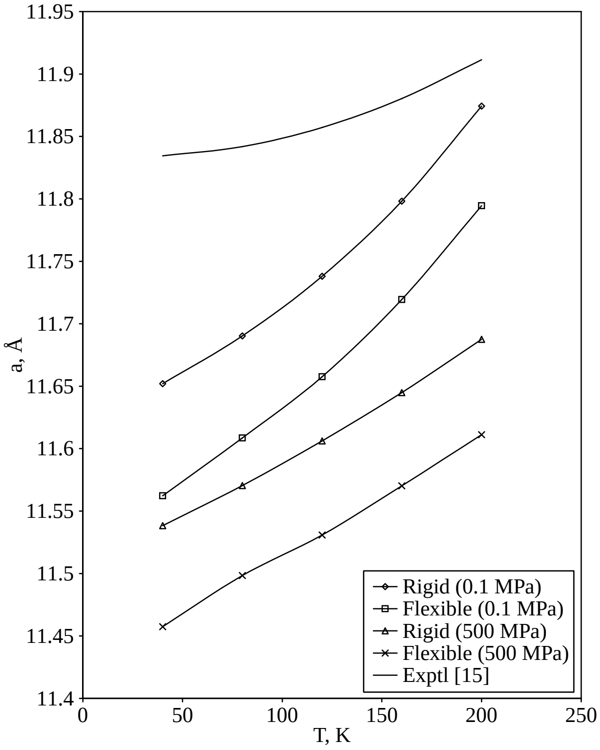

Figure 5. Effect of temperature on the lattice parameter.

4. Conclusions

Considering systems with rigid molecules may result in a substantial saving of computational time and it often avoids a source of error. However, this is not the case of water molecules due to their polarity and their interactions, which strongly depend on their highly directional characteristics such as the vibrational spectra from where the hydrate structure can be deduced. In this work, models for molecular simulation of rigid and flexible structures were compared with those for molecules of water and methane. The tendencies of the thermodynamic properties results agree with those obtained in studies of rigid and flexible liquid water. The positions of the peaks in the radial distribution functions also agree with experimental data in both flexible and rigid models. The height and the form of these peaks indicate the formation of more well-defined structures for the rigid model. However, this result might not be due to the restrictions imposed on the intramolecular mobility effect but to the different dipole moments in the water molecule models. It is ratified here that the van der Waals and Platteeeuw theory should be modified through the inclusion of distortion effects in the lattice to improve the prediction of hydrate formation and phase equilibrium calculations. The effect of the flexibility in the molecules of the hydrate is observed in major measure in the thermodynamic properties and it is less valuable on the structural properties analysed in this work.

References

[1] E.D. Sloan, *Clathrate Hydrates of Natural Gases*, Marcel Dekker Inc., New York, 1998.

[2] H. Jiang, K.D. Jordan, and C.E. Taylor, *Molecular dynamics simulations of methane hydrate using polarizable force fields*, J. Phys. Chem. B 111 (2007), pp. 6486–6492.

[3] V.V. Sizov and E.M. Piotrovskaya, *Computer simulation of methane hydrate cage occupancy*, J. Phys. Chem. B 111 (2007), pp. 2886–2890.

[4] S. Circone, S.H. Kirby, and L.A. Stern, *Direct measurement of methane hydrate composition along the hydrate equilibrium boundary*, J. Phys. Chem. B 109 (2005), pp. 9468–9475.

[5] S. Circone, L.A. Stern, S.H. Kirby, W.B. Durham, B.C. Chakoumakos, C.J. Rawn, A.J. Rondinone, and Y. Ishii, *CO_2 hydrate: Synthesis, composition, structure, dissociation behavior, and a comparison to structure I CH_4 hydrate*, J. Phys. Chem. B 107 (2003), pp. 5529–5539.

[6] J.H. van-der-Waals, and J.C. Platteeuw, *Clathrate solutions*, Adv. Chem. Phys. 2 (1959), pp. 1–57.

[7] A.A. Chialvo, M. Houssa, and P.T. Cummings, *Molecular dynamics study of the structure and thermophysical properties of model sI clathrate hydrates*, J. Phys. Chem. B 106 (2002), pp. 442–451.

[8] P.M. Rodger, *Stability of gas hydrates*, J. Phys. Chem. 94 (1990), pp. 6080–6089.

[9] H.J.C. Berendsen, J.P.M. Postma, W.F. van Gunsteren, and J. Hermans, *Interaction models for water in relation to protein hydration*, In *Intermolecular Forces: Proceedings of the Fourteenth Jerusalem Symposium on Quantum Chemistry and Biochemistry*, Jerusalem (1981).

[10] H.J.C. Berendsen, J.R. Grigera, and T.P. Straatsma, *The missing term in effective pair potentials*, J. Phys. Chem. 91 (1987), pp. 6269–6271.

[11] M.W. Mahoney and W.L. Jorgensen, *A five-site model for liquid water and the reproduction of the density anomaly by rigid, nonpolarizable potential functions*, J. Chem. Phys. 112 (2000), pp. 8910–8922.

[12] W.L. Jorgensen, J.D. Madura, and C.J. Swenson, *Optimized intermolecular potential functions for liquid hydrocarbons*, J. Am. Chem. Soc. 106 (1984), pp. 6638–6646.

[13] P. Ren and J.W. Ponder, *Polarizable atomic multipole water model for molecular mechanics simulation*, J. Phys. Chem. B 107 (2003), pp. 5933–5947.

[14] H. Yu and W.F. van Gunsteren, *Charge-on-spring polarizable water models revisited: From water clusters to liquid water to ice*, J. Chem. Phys. 121 (2004), pp. 9549–9564.

[15] A.G. Ogienko, A.V. Kurnosov, A.Y. Manakov, E.G. Larionov, A.I. Ancharov, M.A. Sheromov, and A.N. Nesterov, *Gas hydrates of argon and methane synthesized at high pressures: Composition, thermal expansion, and self-preservation*, J. Phys. Chem. B 110 (2006), pp. 2840–2846.

[16] W.C. Swope, H.C. Andersen, P.H. Berens, and K.R. Wilson, *A computer simulation method for the calculation of equilibrium constants for the formation of physical clusters of molecules: Application to small water clusters*, J. Chem. Phys. 76 (1982), pp. 637–649.

[17] W.F. van Gunsteren and M. Karplus, *Effect of constraints on the dynamics of macromolecules*, Macromolecules 15 (1982), pp. 1528–1544.

[18] R.K. McMullan and G.A. Jeffrey, *Polyhedral clathrate hydrates. IX. Structure of ethylene oxide hydrate*, J. Chem. Phys. 42 (1965), pp. 2725–2732.

[19] J.D. Bernal and R.H. Fowler, *A theory of water and ionic solution, with particular reference to hydrogen and hydroxyl ions*, J. Chem. Phys. 1 (1933), pp. 515–548.

[20] O.K.R. Førrisdahl, B. Kvamme, and A.D.J. Haymet, *Methane clathrate hydrates: Melting, supercooling and phase separation from molecular dynamics computer simulations*, Mol. Phys. 89 (1996), pp. 819–834.

[21] H.J.C. Berendsen, J.P.M. Postma, W.F. van Gunsteren, A. DiNola, and J.R. Haak, *Molecular dynamics with coupling to an external bath*, J. Chem. Phys. 81 (1984), pp. 3684–3690.

[22] M.P. Allen and D.J. Tildesley, *Computer Simulation of Liquids*, Oxford University Press, New York, 1987.

[23] T.I. Mizan, P.E. Savage, and R.M. Ziff, *Molecular dynamics of supercritical water using a flexible SPC model*, J. Phys. Chem. 98 (1994), pp. 13067–13076.

[24] O. Teleman, B. Jönsson, and S. Engström, *A molecular dynamics simulation of a water model with intramolecular degrees of freedom*, Mol. Phys. 60 (1987), pp. 193–203.

[25] W.L. Jorgensen, D.S. Maxwell, and J. Tirado-Rives, *Development and testing of the OPLS all-atom force field on conformational energetics and properties of organic liquid*, J. Am. Chem. Soc. 118 (1996), pp. 11225–11236.

[26] M. Neumann, *The dielectric constant of water. Computer simulations with the MCY potential*, J. Chem. Phys. 82 (1985), pp. 5663–5672.

[27] H.C.J. Andersen, *Rattle: A velocity version of the shake algorithm for molecular dynamics calculations*, J. Comput. Phys. 52 (1983), pp. 24–34.

[28] J.P. Ryckaert, G. Ciccotti, and H.J.C. Berendsen, *Numerical integration of the Cartesian equations of motion of a system with constraints: Molecular dynamics of* n-*alkanes*, J. Comput. Phys. 23 (1977), pp. 327–341.

[29] A. Wallqvist and O. Teleman, *Properties of flexible water models*, Mol. Phys. 74 (1991), pp. 515–533.

[30] C. Giavarini and F. Maccioni, *Self-preservation at low pressures of methane hydrates with various gas contents*, Ind. Eng. Chem. Res. 43 (2004), pp. 6616–6621.

[31] J. Zhang, S. Piana, R. Freij-Ayoub, M. Rivero, and S.K. Choi, *Molecular dynamics study of methane in water: Diffusion and structure*, Mol. Simul. 32 (2006), pp. 1279–1286.

[32] H. Thompson, A.K. Soper, P. Buchanan, N. Aldiwan, J.L. Creek, and C.A. Koh, *Methane hydrate formation and decomposition: Structural studies via neutron diffraction and empirical potential structure refinement*, J. Chem. Phys. 124 (2006), pp. 164508–164512.

[33] A.K. Soper, *Empirical potential Monte Carlo simulation of fluid structure*, Chem. Phys. 202 (1996), pp. 295–306.

[34] K.C. Hester, Z. Huo, A.L. Ballard, C.A. Koh, K.T. Miller, and E.D. Sloan, *Thermal expansivity for sI and sII clathrate hydrates*, J. Phys. Chem. B 111 (2007), pp. 8830–8835.